Model Order Reduction for Complex Ocular Simulations Inside the Human Eyeball

Thomas Saigre[1], Christophe Prud'homme[1], Marcela Szopos[2]

[1]Institut de Recherche Mathématique Avancée, UMR 7501 Université de Strasbourg et CNRS
[2]Université Paris Cité, CNRS, MAP5, F-75006 Paris, France

SIAM CSE23
28th February 2023

Introduction

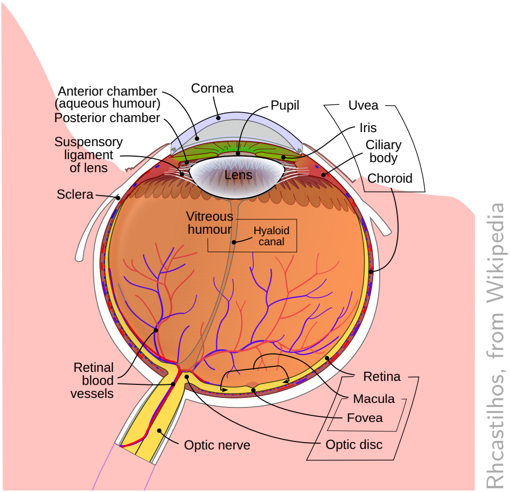

- Need to understand ocular **physiology** and **pathology**,
- **Heat transfer** has an impact on the distribution of drugs in the eye [a],
- Complexity to perform **measurements** on a human subject [b], only on surface [c].

---

[a] Bhandari et al., J. Control Release (2020)
[b] Rosenbluth et al., Exp. Eye Res. (1977)
[c] Purslow et al., Eye Contact Lens (2005)

Introduction

Model complexity

- Monophysics-Multiphysics problem
- Numerous parameters and scarce experimental data
- Influence of multiple risk factors or a combination of them

Introduction

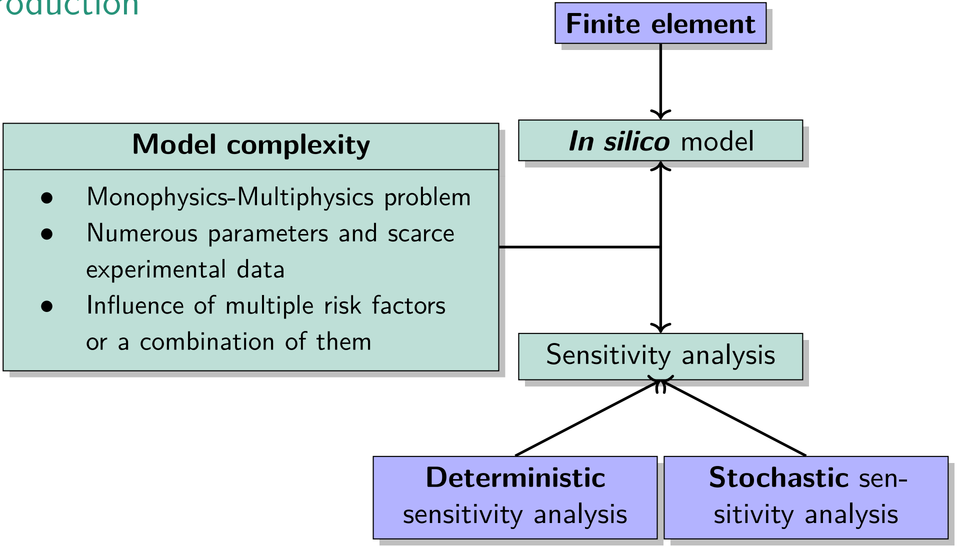

Introduction

Model complexity

- Monophysics-Multiphysics problem
- Numerous parameters and scarce experimental data
- Influence of multiple risk factors or a combination of them

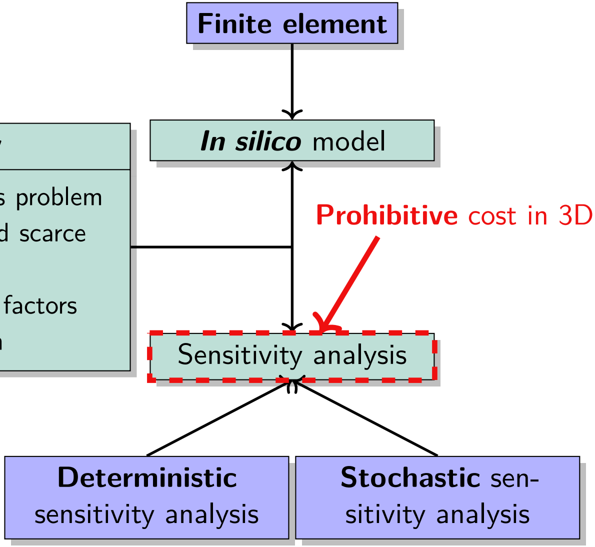

Introduction

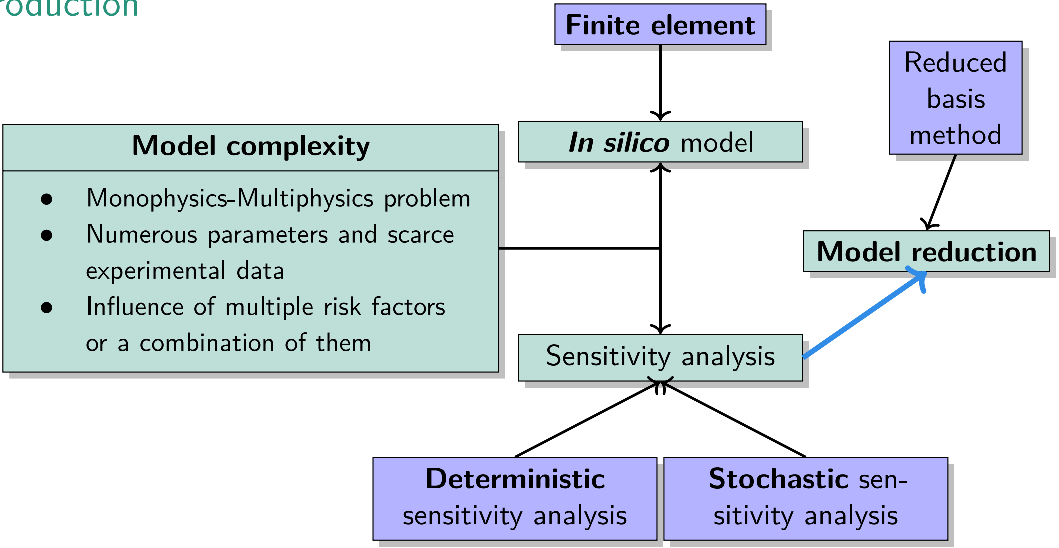

Table of contents

Models

Geometrical model[1]

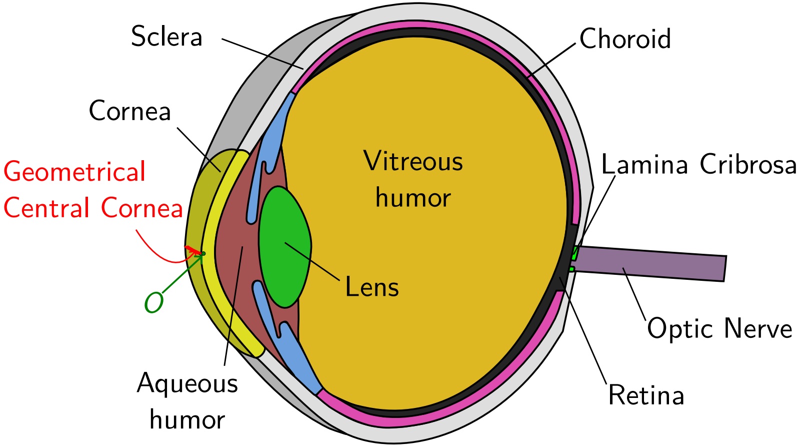

[1] Lorenzo Sala. "Mathematical modelling and simulation of ocular blood flows and their interactions". Theses. Université de Strasbourg, Sept. 2019.

Biophysical model[2]

$$\rho_i C_{p,i} \frac{\partial T_i}{\partial t} + \nabla \cdot (k_i \nabla T_i) = 0 \qquad \text{over } \Omega_i$$

where :

- i is the region index (Cornea, Aqueous Humor, Vitreous Humor, Sclera, Iris, Lens, Choroid, Lamina, Retine, Optic Nerve),
- T_i [K] is the temperature in the volume i,
- t [s] is the time,
- k_i $[\mathrm{W\,m^{-1}} K^{-1}]$ is the thermal conductivity, ρ_i $[\mathrm{kg\,m^{-3}}]$ is the density and $C_{p,i}$ $[\mathrm{J\,kg^{-1}} K^{-1}]$ is the specific heat.

[2] J.A. Scott. "A finite element model of heat transport in the human eye". In: *Physics in Medicine and Biology* 33.2 (1988), pp. 227–242; Ng, E.Y.K. and Ooi, E.H. "FEM simulation of the eye structure with bioheat analysis". In: *Computer Methods and Programs in Biomedicine* 82.3 (2006), pp. 268–276.

Biophysical model

Interface conditions : $\begin{cases} T_i = T_j \\ k_i(\nabla T_i \cdot \underline{n}_i) = -k_j(\nabla T_j \cdot \underline{n}_j) \end{cases}$ over $\partial\Omega_i \cap \partial\Omega_j$

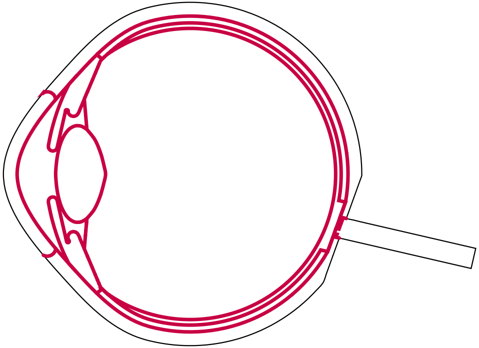

Figure 1: Description of the boundary and interface conditions of the domain

Biophysical model

Robin condition on Γ_N : $-k\dfrac{\partial T}{\partial \underline{n}} = h_{\text{bl}}(T - T_{\text{bl}})$

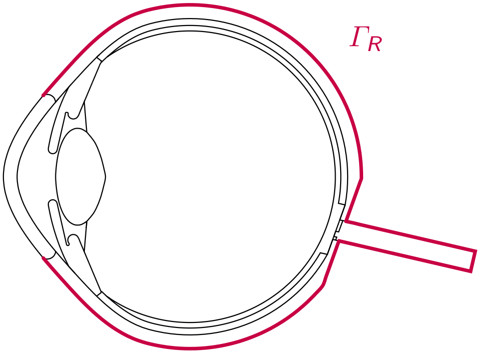

Figure 1: Description of the boundary and interface conditions of the domain

Biophysical model

Linearized Neumann condition[a] on Γ_N : $-k_i \dfrac{\partial T_i}{\partial \underline{n}} = h_{\text{amb}}(T_i - T_{\text{amb}}) + h_r(T_i - T_{\text{amb}}) + E$

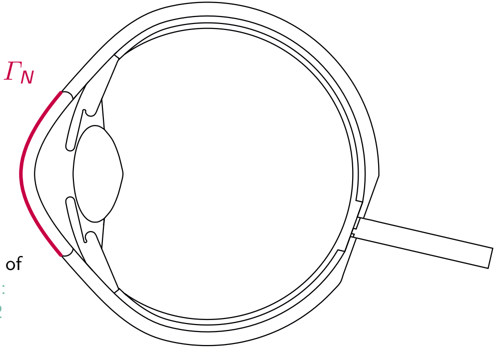

$\longrightarrow$ Model $\mathcal{E}_{\text{lin}}$

$h_r = 6\,\text{W}\text{m}^{-2}\text{K}^{-1}$

[a] J.A. Scott. "A finite element model of heat transport in the human eye". In: *Physics in Medicine and Biology* 33.2 (1988), pp. 227–242

Figure 1: Description of the boundary and interface conditions of the domain

Parameter dependant model

Symbol	Name	Dimension	baseline value
T_{amb}	Ambient temperature	[K]	298
T_{bl}	Blood temperature	[K]	310
h_{amb}	Ambiant air convection coefficient	$[\mathrm{W\,m^{-2}K^{-1}}]$	10
h_{bl}	Blood convection coefficient	$[\mathrm{W\,m^{-2}K^{-1}}]$	65
E	Evaporation rate	$[\mathrm{W\,m^{-2}}]$	40
k_{lens}	Lens conductivity	$[\mathrm{W\,m^{-1}K^{-1}}]$	0.4
k_{cornea}	Cornea conductivity	$[\mathrm{W\,m^{-1}K^{-1}}]$	0.58
k_{sclera}	Sclera conductivity	$[\mathrm{W\,m^{-1}K^{-1}}]$	1.0042
$k_{\text{AqueousHumor}}$	Aqueous humor conductivity	$[\mathrm{W\,m^{-1}K^{-1}}]$	0.28
$k_{\text{VitreousHumor}}$	Vitreous humor conductivity	$[\mathrm{W\,m^{-1}K^{-1}}]$	0.603
ε	Emissivity of the cornea	[–]	0.975

Table 1: Parameters involved in the model

Geometrical parameters may be involved, but we will not consider them in this work.

Present work : focus on parametric analysis

Parameter	Minimal value	Maximal value	Baseline value	Dimension
T_{amb}	283.15	303.15	298	[K]
T_{bl}	308.3	312	310	[K]
h_{amb}	8	100	10	$[\mathrm{W\,m^{-2}}K^{-1}]$
h_{bl}	50	110	65	$[\mathrm{W\,m^{-2}}K^{-1}]$
E	20	320	40	$[\mathrm{W\,m^{-2}}]$
k_{lens}	0.21	0.544	0.4	$[\mathrm{W\,m^{-1}}K^{-1}]$

Table 2: Range of values for the parameters

- We set $\mu = (T_{\mathrm{amb}}, T_{\mathrm{bl}}, h_{\mathrm{amb}}, h_{\mathrm{bl}}, E, k_{\mathrm{lens}}) \in D^{\mu} \subset \mathbb{R}^6$.
- $\bar{\mu} \in D^{\mu}$ is the baseline value of the parameters.

Methods

High fidelity resolution

- Standard Galerkin continuous finite element method, $\mathbb{P}_1$ and $\mathbb{P}_2$ piecewise polynomials,
- Mesh caracteristics :

h	**nDof** $\mathbb{P}_1$	**nDof** $\mathbb{P}_2$
0.47	$2.08 \cdot 10^5$	$1.58 \cdot 10^6$

- Usage of the open-source library Feel++[3] to run simulations

[3] Christophe Prud'homme et al. *feelpp/feelpp: Feel++ V110.2 Released*. Version v0.110.2. Nov. 2022, source code : github.com/feelpp/feelpp.

Model Order Reduction

- **Goal :** replicate input-output behavior of the high fidelity model $\mathcal{E}_{\text{lin}}$ with a reduced order model $\mathcal{E}_{\text{RBM}}$,
- With a procedure stable and efficient.

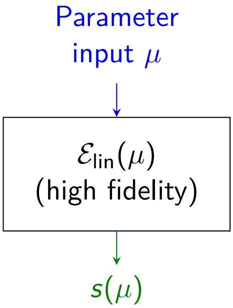

Model Order Reduction

- **Goal :** replicate input-output behavior of the high fidelity model $\mathcal{E}_{\text{lin}}$ with a reduced order model $\mathcal{E}_{\text{RBM}}$,
- With a procedure stable and efficient.

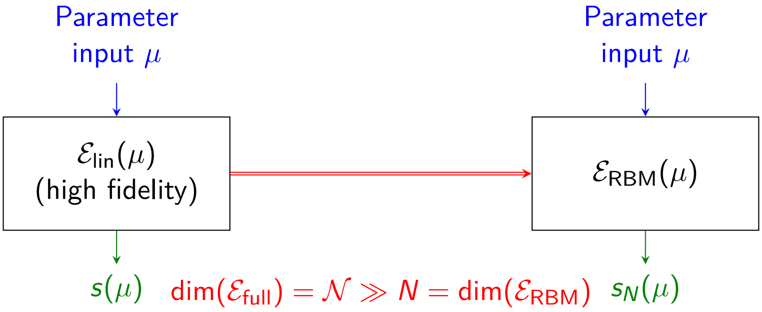

Model Order Reduction[4]

- $\mathcal{E}_{\text{lin}}$: given $\mu \in D^\mu$, evaluate $s(\mu) = \underline{L}(\mu)^T \underline{u}(\mu)$ where $\underline{u}(\mu) \in X^\mathcal{N}$ satisfies the equation :

$$\boldsymbol{A}(\mu)\underline{u}(\mu) = \underline{F}(\mu)$$

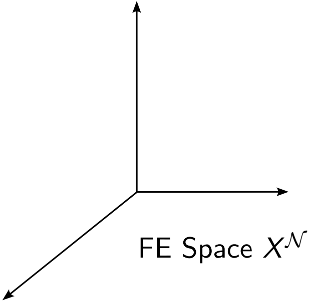

[4] Alfio Quarteroni et al. *Reduced Basis Methods for Partial Differential Equations*. Springer International Publishing, 2016.

Model Order Reduction[4]

- $\mathcal{E}_{\text{lin}}$: given $\mu \in D^\mu$, evaluate $s(\mu) = \underline{L}(\mu)^T \underline{u}(\mu)$ where $\underline{u}(\mu) \in X^\mathcal{N}$ satisfies the equation :

$$\boldsymbol{A}(\mu)\underline{u}(\mu) = \underline{F}(\mu)$$

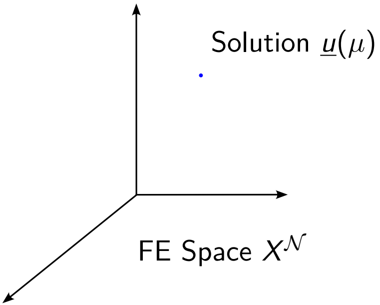

[4] Alfio Quarteroni et al. *Reduced Basis Methods for Partial Differential Equations*. Springer International Publishing, 2016.

Model Order Reduction[4]

- $\mathcal{E}_{\text{lin}}$: given $\mu \in D^\mu$, evaluate $s(\mu) = \underline{L}(\mu)^T \underline{u}(\mu)$ where $\underline{u}(\mu) \in X^\mathcal{N}$ satisfies the equation :

$$\boldsymbol{A}(\mu)\underline{u}(\mu) = \underline{F}(\mu)$$

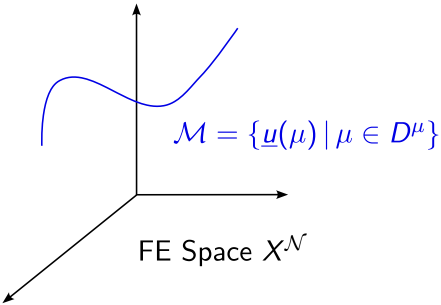

[4] Alfio Quarteroni et al. *Reduced Basis Methods for Partial Differential Equations*. Springer International Publishing, 2016.

Model Order Reduction[4]

- $\mathcal{E}_{\text{lin}}$: given $\mu \in D^\mu$, evaluate $s(\mu) = \underline{L}(\mu)^T \underline{u}(\mu)$ where $\underline{u}(\mu) \in X^\mathcal{N}$ satisfies the equation :

$$\boldsymbol{A}(\mu)\underline{u}(\mu) = \underline{F}(\mu)$$

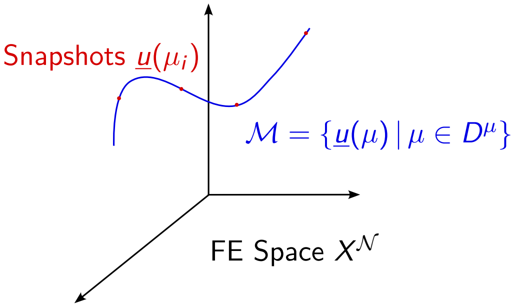

[4] Alfio Quarteroni et al. *Reduced Basis Methods for Partial Differential Equations*. Springer International Publishing, 2016.

Model Order Reduction

- To compute the reduced basis, we take *snapshots* for different μ-values $\mu_1, \cdots, \mu_N$, and define the matrix :

$$\mathbb{Z}_N = [\xi_1, \cdots, \xi_N] \in \mathbb{R}^{\mathcal{N} \times N}$$

where $\xi_i = u(\mu_i)$, is orthonormalized.

- Then, $u(\mu) \approx \sum_{i=1}^{N} \underline{u}_{N,i}(\mu)\xi_i = \mathbb{Z}_N \underline{u}_N$, so the reduced problem is :

$$\underbrace{\mathbb{Z}_N^T \boldsymbol{A}(\mu) \mathbb{Z}_N}_{:=\boldsymbol{A_N}(\mu) \in \mathbb{R}^{N \times N}} \underline{u}_N(\mu) = \underbrace{\mathbb{Z}_N^T \underline{F}(\mu)}_{:=\underline{F}_N(\mu) \in \mathbb{R}^N}$$

$$s_N(\mu) = \underbrace{\underline{L}_N^T(\mu) \mathbb{Z}_N}_{:=\underline{L}_N^T(\mu) \in \mathbb{R}^N} \underline{u}_N$$

Offline / Online decomposition

Offline stage

- We want to write $\boldsymbol{A}(\mu) \approx \sum_{q=1}^{Q_a} \theta_A^q(\mu)\boldsymbol{A}^q$,

  and $\underline{F}(\mu) \approx \sum_{q=1}^{Q_f} \theta_F^q(\mu)\underline{F}^q$.
- Compute and store
  $\boldsymbol{A}_N^q = \underbrace{\mathbb{Z}_N^T \boldsymbol{A}^q \mathbb{Z}_N}_{\text{independent of } \mu}$ and $\underline{F}_N^q = \mathbb{Z}_N^T \underline{F}^q$.
- Obtained through EIM decomposition
- We have $Q_a = 3$ and $Q_f = 2$.

Offline / Online decomposition

Offline stage

- We want to write $\boldsymbol{A}(\mu) \approx \sum_{q=1}^{Q_a} \theta_A^q(\mu) \boldsymbol{A}^q$,

  and $\underline{F}(\mu) \approx \sum_{q=1}^{Q_f} \theta_F^q(\mu) \underline{F}^q$.
- Compute and store
  $\boldsymbol{A}_N^q = \underbrace{\mathbb{Z}_N^T \boldsymbol{A}^q \mathbb{Z}_N}_{\text{independent of } \mu}$ and $\underline{F}_N^q = \mathbb{Z}_N^T \underline{F}^q$.
- Obtained through EIM decomposition
- We have $Q_a = 3$ and $Q_f = 2$.

Online stage

- Independent of finite element dimension,
- $\boldsymbol{A}_N(\mu) = \sum_{q=1}^{Q_a} \theta_A^q(\mu) \boldsymbol{A}_N^q \in \mathbb{R}^{N \times N}$
- $\underline{F}_N(\mu) = \sum_{q=1}^{Q_f} \theta_F^q(\mu) \underline{F}_N^q \in \mathbb{R}^N$

Time of execution

Using the parameter $\mu = \bar{\mu}$ (baseline values) :

	$\mathbb{P}_1$	$\mathbb{P}_2$	Online
$\mathcal{N}$	207 845	1 580 932	$N = 10$
t_{exec}	21.221s	123.92s	0.14 s
relative time	5.84	1	885.1

In the following, $\mathbb{P}_2$ discretization is used for high fidelity resolution.

Verification and validation

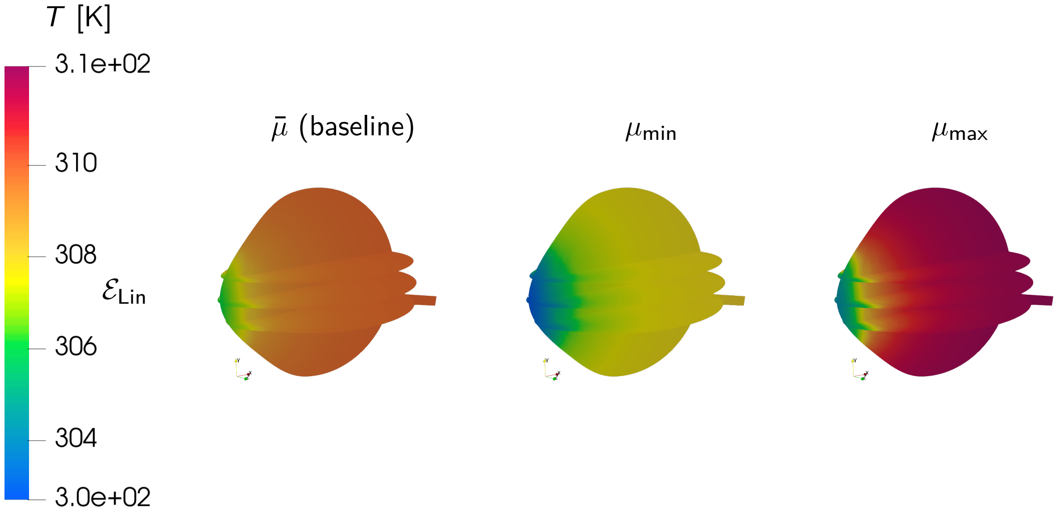
T [K]
3.1e+02
310
308
306
304
3.0e+02
$\mathcal{E}_{\text{Lin}}$
$\bar{\mu}$ (baseline)
μ_{min}
μ_{max}

Comparaison with previous numerical studies

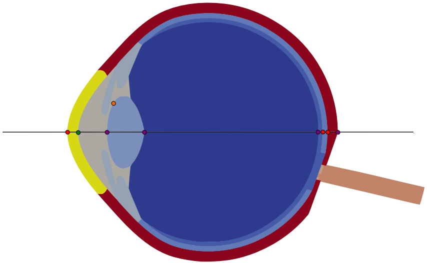

[Sco88] : J.A. Scott. "A finite element model of heat transport in the human eye". In: *Physics in Medicine and Biology* 33.2 (1988), pp. 227–242

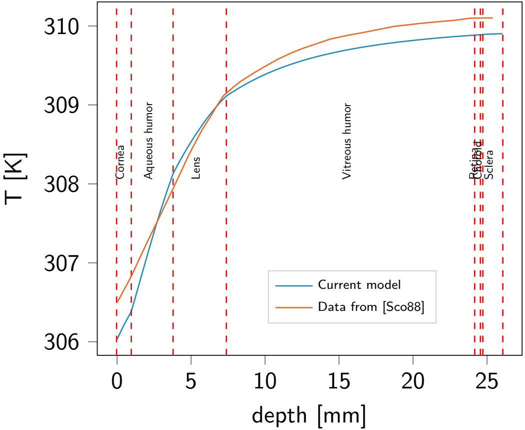

Figure 2: Temperature over an horizontal line

Comparison with experimental values

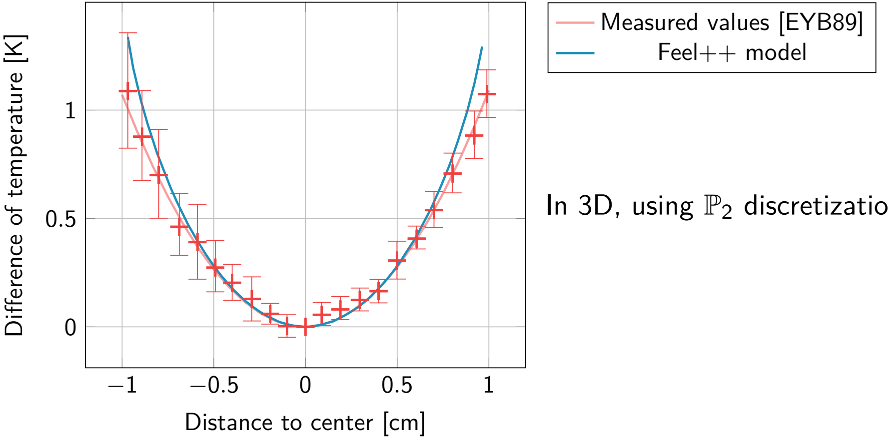

In 3D, using $\mathbb{P}_2$ discretization

Figure 3: Temperature over the GCC

Verification of reduced model, maximal difference : 0.0024 K

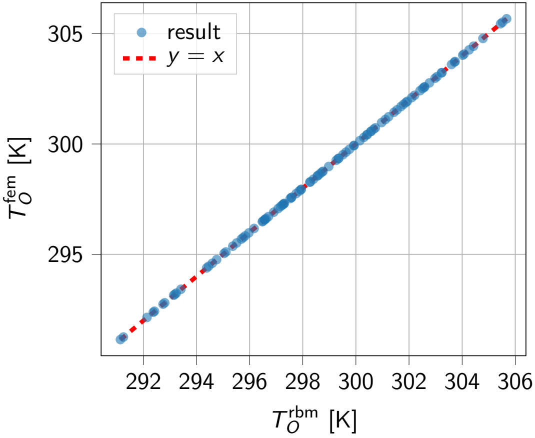

Figure 4: FEM vs RBM output, tested with 100 parameters

Sensitivity analysis

Outputs of interest

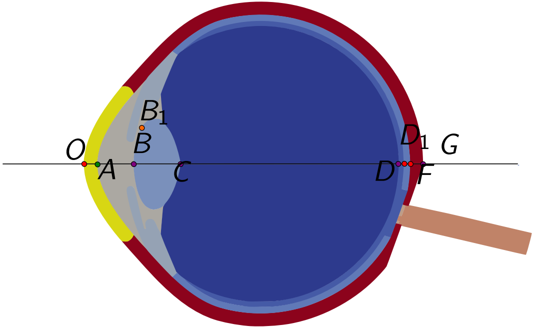

Figure 5: Featured geometrical locations for the outputs of interest (temperature)

Deterministic sensitivity analysis

- We choose one parameter among the 6 parameters of the model,
- We fix the other ones to their baseline value,
- We make the selected parameter vary to study the impact of this single parameter on the output of the model.

Deterministic sensitivity analysis

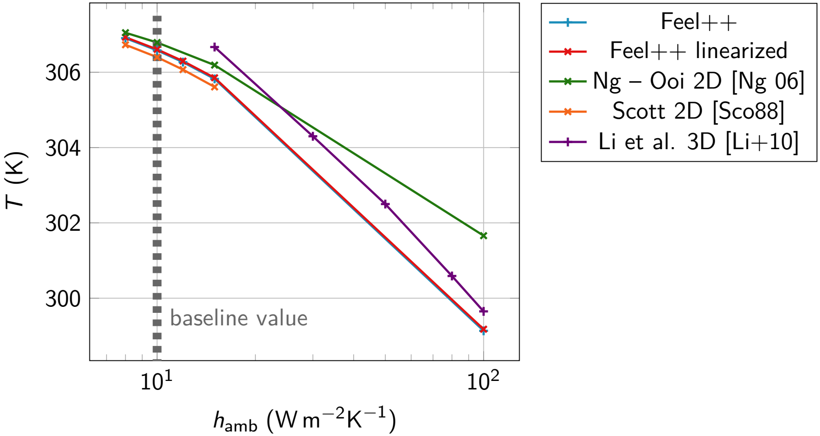

Figure 6: Effect of h_{amb} at point O

Deterministic sensitivity analysis

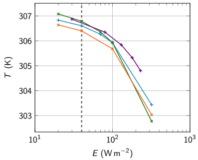

(a) E

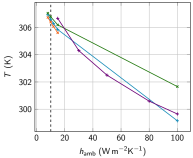

(b) h_{amb}

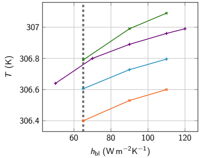

(c) h_{bl}

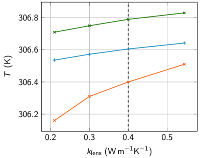

(d) k_{lens}

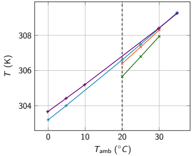

(e) T_{amb}

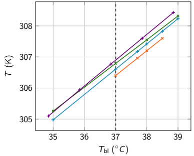

(f) T_{bl}

Figure 6: Point O (Feel++ model, [Ng 06], [Sco88], [Li+10])

Sobol indices

- $\mu = (\mu_1, \ldots, \mu_n) \in D^\mu$,
- $\mu_i \sim X_i$ where $(X_i)_i$ is a familly of *independent* random variables,
- Output $s_N(\mu) \sim Y = f(X_1, \ldots, X_n)$,
- Distributions selected from data available in the literature.

Sobol indices

- **First-order indices**:

$$S_j = \frac{\mathrm{Var}\left(\mathbb{E}\left[Y|X_j\right]\right)}{\mathrm{Var}(Y)} \tag{5.1}$$

- **Total-order indices**:

$$S_j^{\mathrm{tot}} = \frac{\mathrm{Var}\left(\mathbb{E}\left[Y|X_{(-j)}\right]\right)}{\mathrm{Var}(Y)} \tag{5.2}$$

where $X_{(-j)} = (X_1, \ldots, X_{j-1}, X_{j+1}, \ldots, X_n)$.

Stochastic sensitivity analysis

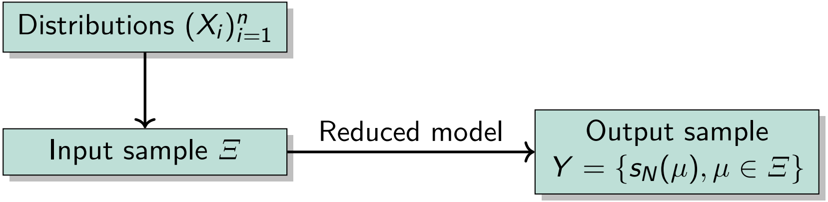

[5] Michaël Baudin et al. "OpenTURNS: An Industrial Software for Uncertainty Quantification in Simulation". In: *Handbook of Uncertainty Quantification*. Ed. by Roger Ghanem et al. Cham: Springer International Publishing, 2016, pp. 1–38.

Stochastic sensitivity analysis

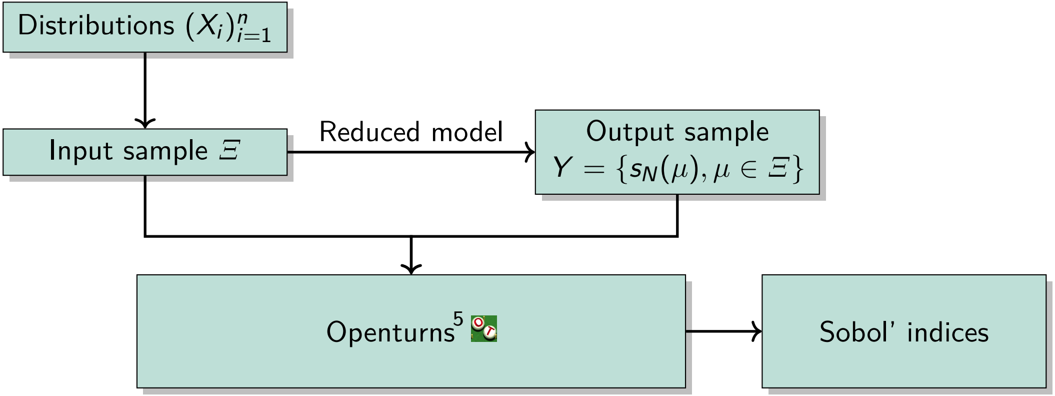

[5] Michaël Baudin et al. "OpenTURNS: An Industrial Software for Uncertainty Quantification in Simulation". In: *Handbook of Uncertainty Quantification*. Ed. by Roger Ghanem et al. Cham: Springer International Publishing, 2016, pp. 1–38.

Stochastic sensitivity analysis

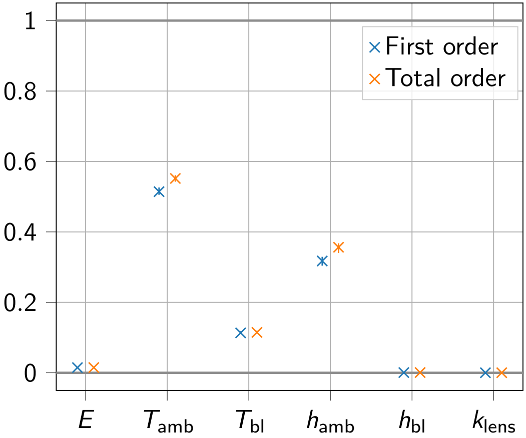

Figure 7: Sobol indices for the SSA : temperature at point O

Stochastic sensitivity analysis

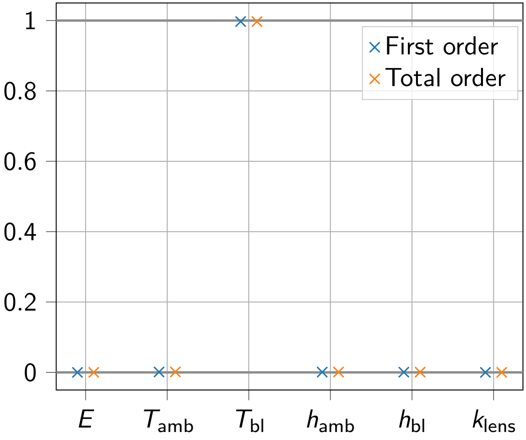

Figure 7: Temperature at point G

Conclusion and outlooks

- Heat transport model in the human eye : FEM simulations, validation against experimental data, and model order reduction,
- **Sensitivity analysis :**
  - **Deterministic** approach : literature comparaison, confirm significant impact of E, h_{amb}, T_{amb} on T_O
  - **Stochastic** approach : computation of Sobol indices thanks to MOR, highlight of the impact of T_{amb} and h_{amb} on T_O. k_{lens} has not impact on any output an can be removed from the parameteric model.

Conclusion and outlooks

Next steps :

- Derive ***a posteriori*** **error estimator** for the reduced model in the case of the 4th order polynomial nonlinearity,
- **Model** : couple thermal effect with aqueous humor dynamics in the anterior chamber,
- **Application** : robust framework to simulate drug delivery in the eye.

References I

[Bau+16] Michaël Baudin et al. "OpenTURNS: An Industrial Software for Uncertainty Quantification in Simulation". In: *Handbook of Uncertainty Quantification*. Ed. by Roger Ghanem, David Higdon, and Houman Owhadi. Cham: Springer International Publishing, 2016, pp. 1–38.

[BBS20] Ajay Bhandari, Ankit Bansal, and Niraj Sinha. "Effect of aging on heat transfer, fluid flow and drug transport in anterior human eye: A computational study". In: *Journal of Controlled Release* 328 (2020), pp. 286–303.

[EYB89] Nathan Efron, Graeme Young, and Noel A Brennan. "Ocular surface temperature.". In: *Current eye research* 8 9 (1989), pp. 901–6.

References II

[Li+10] Eric Li et al. "Modeling and simulation of bioheat transfer in the human eye using the 3D alpha finite element method (αFEM)". In: *International Journal for Numerical Methods in Biomedical Engineering* 26.8 (2010), pp. 955–976.

[Ng 06] Ng, E.Y.K. and Ooi, E.H. "FEM simulation of the eye structure with bioheat analysis". In: *Computer Methods and Programs in Biomedicine* 82.3 (2006), pp. 268–276.

[NO07] E.Y.K. Ng and E.H. Ooi. "Ocular surface temperature: A 3D FEM prediction using bioheat equation". In: *Computers in Biology and Medicine* 37.6 (2007), pp. 829–835.

[Pru+22] Christophe Prud'homme et al. *feelpp/feelpp: Feel++ V110.2 Released*. Version v0.110.2. Nov. 2022.

References III

[PW05] Christine Purslow and James S Wolffsohn. "Ocular surface temperature: a review". en. In: *Eye Contact Lens* 31.3 (May 2005), pp. 117–123.

[QMN16] Alfio Quarteroni, Andrea Manzoni, and Federico Negri. *Reduced Basis Methods for Partial Differential Equations*. Springer International Publishing, 2016.

[RF77] Robert F. Rosenbluth and Irving Fatt. "Temperature measurements in the eye". In: *Experimental Eye Research* 25.4 (1977), pp. 325–341.

[Sal19] Lorenzo Sala. "Mathematical modelling and simulation of ocular blood flows and their interactions". Theses. Université de Strasbourg, Sept. 2019.

[Sco88] J.A. Scott. "A finite element model of heat transport in the human eye". In: *Physics in Medicine and Biology* 33.2 (1988), pp. 227–242.

Thanks for your attention !

Parameter dependant model

Values of the parameters from the litterature :

- J.A. Scott. "A finite element model of heat transport in the human eye". In: *Physics in Medicine and Biology* 33.2 (1988), pp. 227–242
- Ng, E.Y.K. and Ooi, E.H. "FEM simulation of the eye structure with bioheat analysis". In: *Computer Methods and Programs in Biomedicine* 82.3 (2006), pp. 268–276
- E.Y.K. Ng et al. "Ocular surface temperature: A 3D FEM prediction using bioheat equation". In: *Computers in Biology and Medicine* 37.6 (2007), pp. 829–835
- Eric Li et al. "Modeling and simulation of bioheat transfer in the human eye using the 3D alpha finite element method (αFEM)". In: *International Journal for Numerical Methods in Biomedical Engineering* 26.8 (2010), pp. 955–976

Linearization

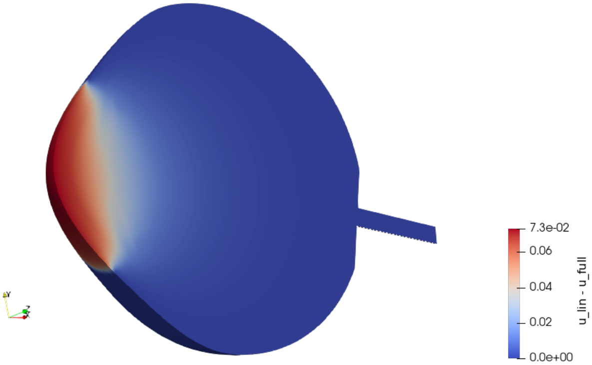

Figure 8: Difference of the temperature between the full model and the linearized model (in K), maximal value : $2.64 \cdot 10^{-2}$ K

How to choose the snapshots ?

Residual error

Let $\mu \in D^{\mu}$. We set $u(\mu)$ the FEM solution, and $u_N(\mu)$ the reduced solution.
We define the residual error as $e(\mu) = u(\mu) - u_N(\mu)$ that satisfies

$$(e(\mu), v)_V = f(v) - a(u_N(\mu), v; \mu) \qquad \forall v \in V$$

How to choose the snapshots ?

Residual error

Let $\mu \in D^\mu$. We set $u(\mu)$ the FEM solution, and $u_N(\mu)$ the reduced solution. We define the residual error as $e(\mu) = u(\mu) - u_N(\mu)$ that satisfies

$$(e(\mu), v)_V = f(v) - a(u_N(\mu), v; \mu) \qquad \forall v \in V$$

$$\widehat{e}(\mu) = \sum_p \theta_F^p(\mu)\mathcal{S}^p + \sum_q \sum_n \theta_A^q(\mu) u_N^n(\mu) \mathcal{L}^{n,q} \tag{7.1}$$

with :

$$\begin{aligned} (\mathcal{S}^p, v) &= f^p(v) && \forall v \in X, \forall p \in [\![1, Q_F]\!] \\ (\mathcal{L}^{n,q}, v) &= -a^q(\xi^n, v) && \forall v \in X, \forall n \in [\![1, N]\!], \forall q \in [\![1, Q_A]\!] \end{aligned} \tag{7.2}$$

Norm of the residual error

$$\|\widehat{e}(\mu)\|_X^2 = (\widehat{e}(\mu), \widehat{e}(\mu))_X$$
$$= \left(\sum_p \theta_F^p S^p + \sum_q \sum_n \theta_A^q u_N^n \mathcal{L}^{n,q}, \sum_p \theta_F^p S^p + \sum_q \sum_n \theta_A^q u_N^n \mathcal{L}^{n,q} \right)_X$$

$$\|\widehat{e}(\mu)\|_X^2 = \sum_p \sum_{p'} \theta_F^p \theta_F^{p'} (\mathcal{S}^p, \mathcal{S}^{p'})_X + 2 \sum_p \sum_q \sum_n \theta_F^p \theta_A^q u_N^n (\mathcal{S}^p, \mathcal{L}^{n,q})_X$$
$$+ \sum_q \sum_n \sum_{q'} \sum_{n'} \theta_A^q \theta_A^{q'} u_N^n u_N^{n'} (\mathcal{L}^{n',q'}, \mathcal{L}^{n,q})_X$$

Greedy algorithm

Algorithm 1: Greedy algorithm

Input: $\mu_0 \in D^\mu$ and $\Xi_{\text{train}} \subset D^\mu$

$S \leftarrow [\mu_0]$

while $\Delta_N^{max} > \varepsilon$ **do**

$\mu^\star \leftarrow \underset{\mu \in \Xi_{\text{train}}}{\arg\max} \|\widehat{e}(\mu)\|_V^2$ (and $\Delta_N^{\max} \leftarrow \max_{\mu \in \Xi_{\text{train}}} \|\widehat{e}(\mu)\|_V^2$)

Append $\mu^\star$ to S

$u(\mu^\star) \leftarrow$ FE solution, using S as generating sample

$\mathbb{Z}_N \leftarrow \{\xi = u(\mu^\star)\} \cup \mathbb{Z}_{N-1}$

end

Output: sample S, reduced basis $\mathbb{Z}_N$

Deterministic sensitivity analysis (more results)

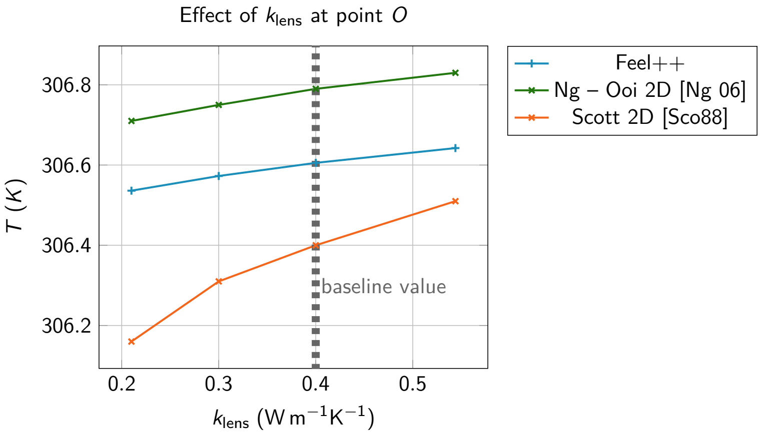

Figure 9: Effect of k_{lens} at point O

Deterministic sensitivity analysis (more results)

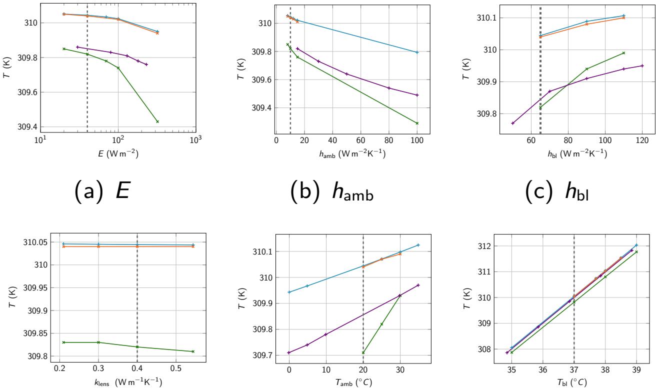

(a) E (b) h_{amb} (c) h_{bl}

(d) k_{lens} (e) T_{amb} (f) T_{bl}

Figure 9: Point G (Feel++ model, [Ng 06], [Sco88], [Li+10])

Distributions

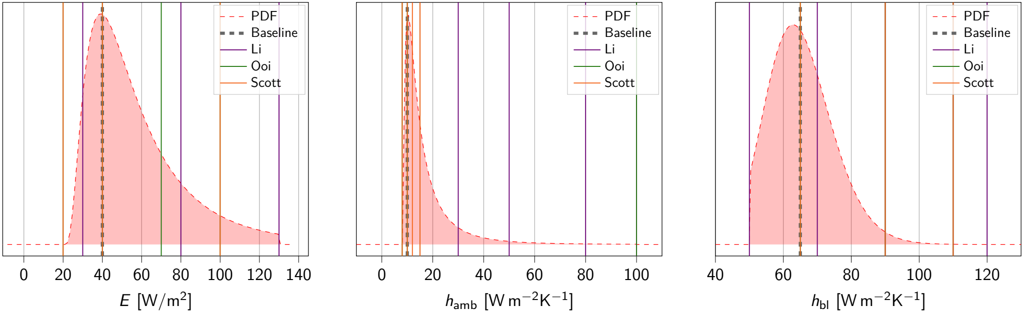

(a) Distribution of E (b) Distribution of h_{amb} (c) Distribution of h_{bl}

Figure 10: Distributions of the parameters. The colored vertical lines represent the values chosen in literature for the DSA

Distributions

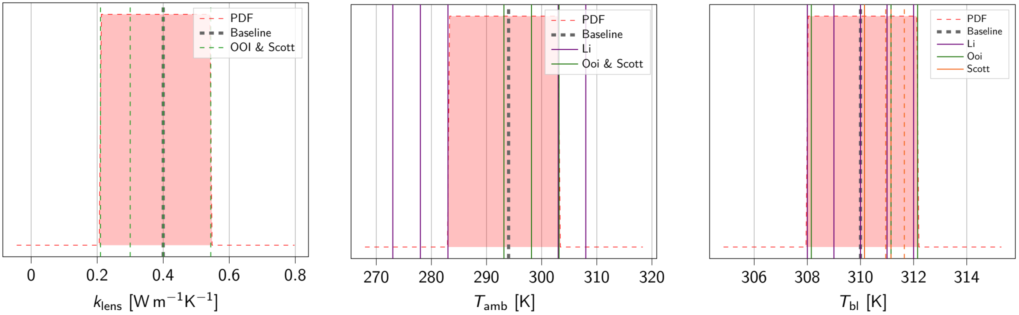

(a) Distribution of k_{lens} (b) Distribution of T_{amb} (c) Distribution of T_{bl}

Figure 10: Distributions of the parameters. The colored vertical lines represent the values chosen in literature for the DSA

Stochastic sensitivity analysis

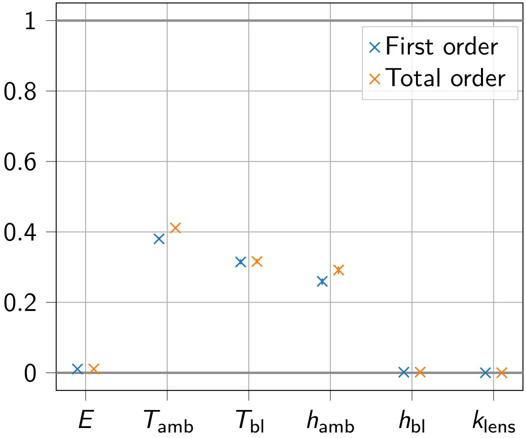

Figure 11: Sobol indices for cornea

Stochastic sensitivity analysis

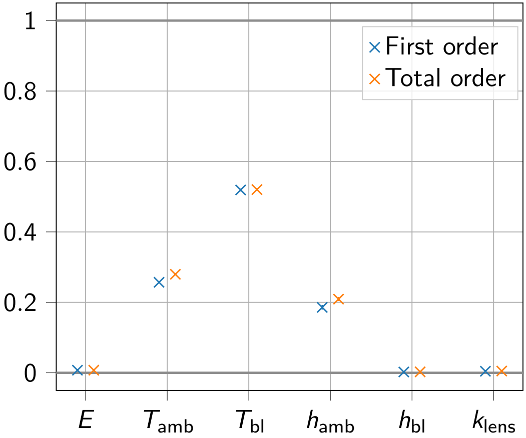

Figure 11: Sobol indices for B1

Stochastic sensitivity analysis

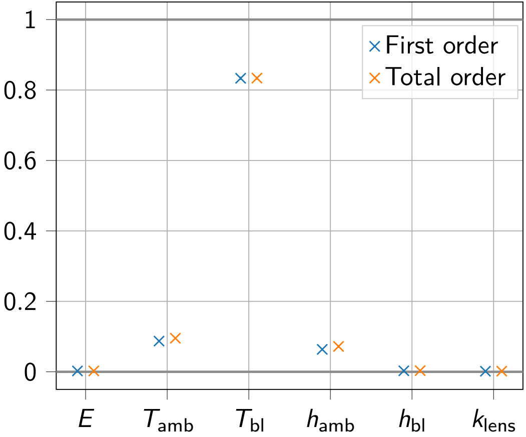

Figure 11: Sobol indices for C

Stochastic sensitivity analysis

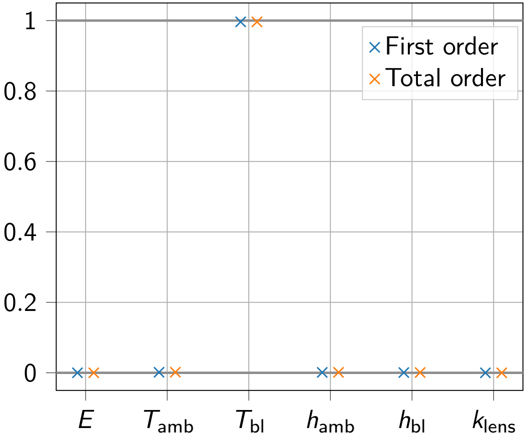

Figure 11: Sobol indices for D1

Stochastic sensitivity analysis

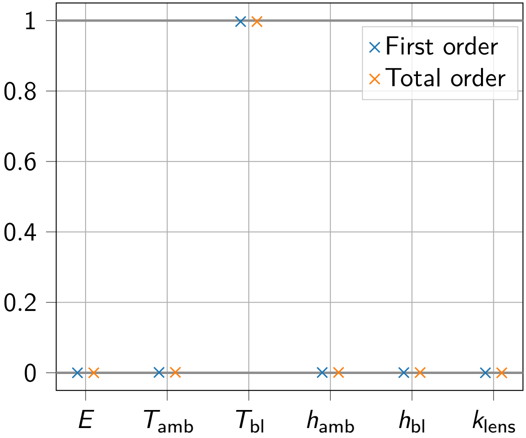

Figure 11: Sobol indices for G